

# WIND EXTRACTION USING SATELLITE IMAGES IN CPTEC: NEW VERSION AND EVALUATION WITH WETAMC/LBA AND OPERATIONAL DSA/CPTEC DATA

Henri Laurent<sup>1,4</sup>, Nelson Arai<sup>2</sup>, Boris Fomin<sup>3</sup>, Luiz Augusto T. Machado<sup>1</sup>  
and Marigliaudio A. Gondim<sup>2</sup>

<sup>1</sup> CTA/IAE/ACA, São José dos Campos, SP

<sup>2</sup> CPTEC/INPE, Cachoeira Paulista, SP

<sup>3</sup> LCP/MSK, Moscow, Russia

<sup>4</sup> IRD, LTHE, Grenoble, France

## ABSTRACT

Wind fields obtained through clouds displacement observed in geostationary satellite images are important tools in the data production for assimilation in atmospheric general circulation models. This study introduces changes in the algorithm and improvements in the method in operation in CPTEC (Center for Weather Forecast and Climatic Studies). Two main improvements were implemented: a clouds semi-transparency height correction, using a new simplified radiative transfer model and a space consistency test. The radiative model performance was evaluated using calculations line by line.

The entire wind derivation scheme was compared with the “state of the art” represented by the wind fields obtained by cloud displacement produced by NOAA/NESDIS, and validated through the comparison with radiosonde data obtained in the campaign WETAMC/LBA. The results show that the products obtained by the CPTEC version have a similar performance as the NOAA/NESDIS products for high tropospheric levels, while indicate the need for more efforts in the determination of middle and low level winds. This new version of the algorithm has been used operationally in CPTEC since September 2000 and some comparisons with radiosonde data are introduced. The results showed that in an operational outline the results were worse than those obtained in campaign, due to problems found in the images and in radiosonde data.

## 1. Introduction

The winds obtained from cloud displacement, observed in geostationary satellite images, are recognized as an important information source for numerical weather prediction models. Wind vectors obtained through these methods are large in number and more important in tropical regions where the conventional observations are sparse. We stress also the importance of this kind of information over the Oceans and mainly in Southern Hemisphere mostly cover by oceans.

Nowadays there are some meteorological centers which operate such models, as EUMETSAT (European Meteorology Satellite) in Europe, NOAA/NESDIS (National Environmental Satellite and Information Data Services) in USA and JMA (Japan Meteorological Agency) in Japan.

The satellite data assimilation as input for the CPTEC forecast model is a fundamental point, mostly for our region where conventional data coverage is sparse. The operational routines implantation for wind extraction, temperature and humidity profiles, precipitation and other diagnostic parameters will enable a more realistic representation of the initial conditions. CPTEC needs to prepare the initial conditions, blending the result of it's own model with other parameters, needing conventional data and others extracted from satellite images.

The geostationary GOES satellite positioned in 75°W observes the earth with images in the visible, infrared and water vapor channels. The spatial resolution is 4 km x 4 km in the infrared channel (IR) and 4 km x 8 km in the water vapor channel (WV). The temporal resolution is 30 minutes for all channels. The model uses nowadays IR and WV images, however it is expected to use in the future visible images to get more precise cloud classification. The model uses one IR image in  $t_0-30$  minutes, one IR and WV images in  $t_0$  and other IR image in  $t_0+30$  minutes. The model operates with the images recorded by the CPTEC acquisition system. This system calibrates and transforms the IR and WV images in radiance values and afterwards in brightness temperature, and navigate the image allowing to obtain the latitudes and longitudes of each pixel.

## 2. Vectors Calculation

The vectors calculation is entirely automatic. A vector is obtained through the displacement of a target (cloud) between two images. For this calculation the model estimate the vectors through the Euclidian distance between a target area of 32x32 pixels (~150 km x 150 km) in the image ( $t$ ) and all the areas of 32x32 pixels which are present in a window of 96x96 pixels in the image ( $t+\Delta t$ ). The method formulations and details were introduced by Laurent and Machado (1994).

### 2.1 Quality Control

For calculated wind quality control analysis, several tests are applied. Obtained the best displacement, the corresponding correlation is calculated to analysis the quality in the target identification. If the correlation is lower than 0.7, the vector is rejected. Other rejection condition is for speed smaller than  $3 \text{ ms}^{-1}$ , because in this case the target can be the surface or a stationary orographic cloud.

The most important quality test is the temporal consistency test. For the application of this test image in  $t_0 -30$  minutes is used. The test calculates the wind vector between  $t_0$  and  $t_0-30$  minutes, the result of calculated vector can not be very different from that calculated between  $t_0$  and  $t_0+30$  minutes. Occuring a significant difference the vector is rejected, because it is considered that the correlation was based in aleatory clouds formations and not in a real displacement of clouds. For this, we use as maximum value applied to the module of difference vector between  $V_1$  (vector between  $t_0$  and  $t_0+30$  minutes) and  $V_2$  (vector between  $t_0-30$  and  $t_0$ ) the following relation:

$$|V_1-V_2| < 5 + 0.2 |V_1| \quad (\text{ms}^{-1})$$

A new test was implemented in this work, to verify the spatial consistency of the vector field. It is applied after the vectors calculation because the wind field is necessary. For each vector  $V_1$  one calculates the vectorial differences with every neighboring vector, in a radius of 4 degrees and in a layer of 100 hPa. Be  $\Delta V$  the minor vector difference, the vector  $V_1$  will be rejected if it does not attend the following relation:

$$|\Delta V| < 1.5 (0.2 |V_1| + 1) \quad (\text{ms}^{-1})$$

The effect of this space consistency test is evaluated in this work.

### 2.2 Wind Vector Height Assignment

It is considered that the pressure level of a given vector the pressure level where the atmosphere temperature is equal to the cloud infrared brightness temperature, using the temperature and pressure profiles from the CPTEC model for the vector geographical position. However, as emissivity of the clouds is often lowering than 1, a correction for semi-transparent clouds is needed. To use this well known “semi-transparency correction” (Bowen and Saunders, 1984, Schmetz et al., 1993) cloud radiances for clear sky are necessary for infrared (IR) and vapor vapour (WV) channels. Thus, it is calculated the average between the 20% colder pixels and the 10% hotter pixels in the calculation

window, for IR and WV images. In parallel a radiative model calculates IR and WV radiances for opaque clouds (emissivity equal to 1) in several heights, using as input data vertical temperature and humidity profiles from the CPTEC model. The radiative model was developed by Fomin (1995) and adapted for the CPTEC wind calculation using GOES IR and WV channels.

### 3. Radiative Model

Firstly, it was used a model line-by-line model (LBL) for radiance simulation in each channel (IR and WV), for several atmosphere profiles, supposing opaque clouds in different levels. Transmittance functions of each channel were adjusted for the IR and WV channels of the GOES-8 satellite. To calculate the absorption coefficients, we use the Fomin's (1995) LBL algorithm, HITRAN-96's spectral database (Rothman et al., 1998) and the water vapor continuum model CKD2.2 (Clough et al., 1989). This model was used with a spectral resolution of  $1/2048 \text{ cm}^{-1}$ , enough to solve each spectral line. The formulations and details used for the integration in the wave number and in the space are presented in Feigelson et al. (1991). The calculations performed by the model LBL included absorption for H<sub>2</sub>O, CO<sub>2</sub>, O<sub>3</sub>, O<sub>2</sub>, CH<sub>4</sub>, N<sub>2</sub>O and CO. The results (not shown) show, as expected, that the absorption by the water vapor is the primordial factor in this case.

In the operational model the atmosphere is divided in N layers where the spectral absorption coefficients are constant and the height has a linear dependence with Planck's function inside the layer (see for example, Ridgway et al., 1991). For the IR channel the radiative equations are solved using the water vapor continuum model proposed by Roberts et al. (1976). For the WV channel, operating in the water vapor strong absorption band, the parameterization was based in the methodology called K-distribution (Liou, 1992) adapted for the water vapor absorption (Chou and Lee, 1996). In this methodology the absorption spectrum  $K_v$ , in this continuous part, can be substituted by a series of M absorption coefficients  $K_i(P,T)$  depending on the pressure and temperature, weighted by weights  $f_i$ . According Chou and Lee (1996) the coefficients  $K_i^*$  (and the weights  $f_i$ ) were derived for the standard  $P_{ref}=300 \text{ hPa}$  and  $T_{ref}=240 \text{ K}$  directly from the LBL data (Liou, 1992). The dependence with the pressure and the temperature can be approached by :

$$K_i(P,T) = R(P,T) K_i^*$$

$$\text{Where } R(P,T) = (P/P_{ref})^\gamma \exp(0.00135(T-T_{ref})).$$

But we change the value  $\gamma=0.8$  suggested by Chou and Lee (1996) for  $\gamma=0.4$ , because they introduced better results for our data kind. We find also that seven coefficients and weights ( $M=7$ ) were enough for a good approach. The values of these coefficients are presented in the Table 1.

i	1	2	3	4	5	6	7
$K_i^*$	10.36151	43.63581	183.7652	773.8973	3259.144	13725.36	57802.14
$F_i$	0.185782	0.2438068	0.1364989	0.07072695	0.03578541	0.01713742	0.005009667

**Table 1.** K - coefficients  $K_i^*$  and weights  $f_m$  used for radiance calculations with K-distribution methodology in GOES-8 WV channel.

The operational model (simplified model) was validated with LBL (exact). Table 2 shows the results for a tropical atmosphere standard profile. The operational model performance is similar to the LBL model using only the H<sub>2</sub>O absorption (errors of 0.1 K in the IR and 0.2 K in WV). Comparing with LBL results using the absorption of seven gases, the operational model errors are lower than 0.5 K in the two channels.

Cloud top (km) T(K)		IR Channel			WV Channel		
		LBL H <sub>2</sub> O	LBL 7-gases	OPER H <sub>2</sub> O	LBL H <sub>2</sub> O	LBL 7-gases	OPER H <sub>2</sub> O
1.0	293.7	292.2	291.9	292.3	243.5	243.5	243.7
2.0	287.7	287.2	286.9	287.2	243.5	243.5	243.7
3.0	283.7	283.5	283.2	283.4	243.5	243.5	243.7
4.0	277.0	276.9	276.8	276.9	243.5	243.5	243.7
5.0	270.3	270.3	270.2	270.3	243.5	243.4	243.6
6.0	263.6	263.6	263.6	263.6	243.2	243.1	243.3
7.0	257.0	257.1	257.0	257.0	242.3	242.3	242.4
8.0	250.3	250.4	250.3	250.3	240.5	240.4	240.6
9.0	243.6	243.7	243.6	243.6	237.5	237.4	237.6
10.0	237.0	237.1	237.1	237.0	233.4	233.4	233.6
11.0	230.1	230.1	230.1	230.1	228.2	228.2	228.4
12.0	223.6	223.6	223.7	223.6	222.8	222.8	222.9
13.0	217.0	217.0	217.1	217.0	217.0	217.0	217.0
14.0	210.3	210.3	210.4	210.3	211.1	211.1	210.9
15.0	203.7	203.7	203.8	203.7	205.2	205.3	204.9

**Table 2.** Brightness temperature (K) for tropical atmosphere with opaque clouds using LBL or operational (OPER) methods. In LBL was used only absorption by H<sub>2</sub>O or absorption by H<sub>2</sub>O+CO<sub>2</sub>+O<sub>3</sub>+O<sub>2</sub>+CH<sub>4</sub>+ N<sub>2</sub>O +CO (7-gas). OPER uses only absorption by H<sub>2</sub>O.

#### 4. Methodology Evaluation

In this part, the wind vectors produced by the new version of the algorithm is analysed in order to evaluate:

- the impact of semi-transparency correction;
- the impact of the spatial consistency test;
- the general quality of the final product.

The evaluation was performed with radiosonde data, obtained during the experiment WETAMC (Amazon Mesoscale Campaign – Wet season) of the LBA (Large scale Biosphere Atmosphere experiment) experiment, where intensive measurements were done (4 radiosondes every 3 hour) from January 15 to February 25, 1999 in Amazonian's area (Silva Dias, 2001, Silva Dias et al., 2001). The results are presented for the period from 11/01/2000 to 28/02/2000.

Besides radiosonde data, the derived winds are compared with the wind vectors produced by NOAA/NESDIS from the same GOES images. This kind of product are being developed for several years, using very sophisticated algorithms (Menzel et al., 1983, Nieman et al., 1997). Considered as one of the two best wind products from satellite (see for example Eumetsat, 1998) it can serve as reference in this area.

The wind vectors were produced for this test version with an average frequency of 3 hours in the study period using the methodology described above, but the temperature and humidity profiles used were from reanalysis data from NCEP (Kalnay et Al., 1996) instead of the CPTEC model data. NCEP reanalysis data are available over a grid of 2.5 latitude and longitude degrees, each 6 hours, for 14 levels : 1000, 925, 850, 700, 600, 500, 400, 300, 250, 200, 150, 100, 70 and 50 hPa. Unfortunately the humidity values in the high troposphere are not well represented; in consequence there are no humidity data for pressure levels smaller than 300 hPa. For these levels the humidity values were interpolated in the following way: a relative humidity linear interpolation between 300 hPa value and 0% at 50 hPa. This approach is reasonable related to radiosonde observations of LBA.

The wind vectors generated from CPTEC were compared with a reference (radiosonde or NOAA/NESDIS vectors) considering a radius of 150 km and a maximum time interval of 1 - 5 hour.

Mean difference vector were calculated between CPTEC vector and the reference vector, as well as the root mean square (RMS) of the mean difference vector, the mean error (BIAS) of the velocity (CPTEC minus reference), the RMS of the velocity difference, the mean reference velocity, and the sample size.

Table 3 shows the results of the comparison between CPTEC and NOAA/NESDIS vectors. Besides the statistical parameters described above the BIAS and the RMS of the pressure difference were calculated. RMS of the mean vector difference is smaller than  $6.5 \text{ ms}^{-1}$ , which is an excellent result because is in the same order of the RMS due to the space and time position differences between vectors (this subject is detailed by Schmetz et al., 1983). The BIAS is also small, and negative as foreseen, because the NOAA/NESDIS vectors speed is artificially increased to compensate for a well-known tendency of satellite estimates in underestimating strong winds. For the vector pressure levels estimates, pressure RMS and BIAS show satisfactory result for the high levels ( $P < 400 \text{ hPa}$ ), however for the middle and low levels high value of BIAS and RMS are observed.

CPTEC x NOAA/NESDIS				
	All levels	P > 700 hPa	400 < P < 700 hPa	P < 400 hPa
Difference Mean Vector	1.5	1.4	1.5	1.7
Difference Mean Vector RMS	6.3	6.1	6.3	6.4
Velocity BIAS	-0.4	-0.2	-0.3	-0.5
Velocity Difference RMS	3.6	3.2	3.6	3.8
Reference Mean velocity	10.2	9.9	10.2	10.5
Pressure BIAS	13	33	24	-2
Pressure RMS	150	190	195	95
Sample size	64593	15175	18498	30920

**Table 3.** Wind (m/s) and pressure (hPa) statistical differences between CPTEC and NOAA/NESDIS vectors. BIAS is the mean difference and RMS is the root mean square.

Notice that the NOAA/NESDIS vectors height is adjusted using a forecast model and/or available observation data. Certainly a better cloud classification is necessary to improve the wind estimate by satellite.

Semi-transparent clouds effect correction in the wind vector height estimate can be obtained comparing the values in Table 4 with the values from Table 3.

CPTEC (without semi-transparency correction) x NOAA/NESDIS				
	All levels	P > 700 hPa	400 < P < 700 hPa	P < 400 hPa
Pressure BIAS	40	35	59	28
Pressure RMS	169	194	210	102
Sample size	64593	15231	22289	27073

**Table 4.** Same as Table.3, but CPTEC vectors were calculated without cloud semi-transparency correction. Only statistics for pressure are presented.

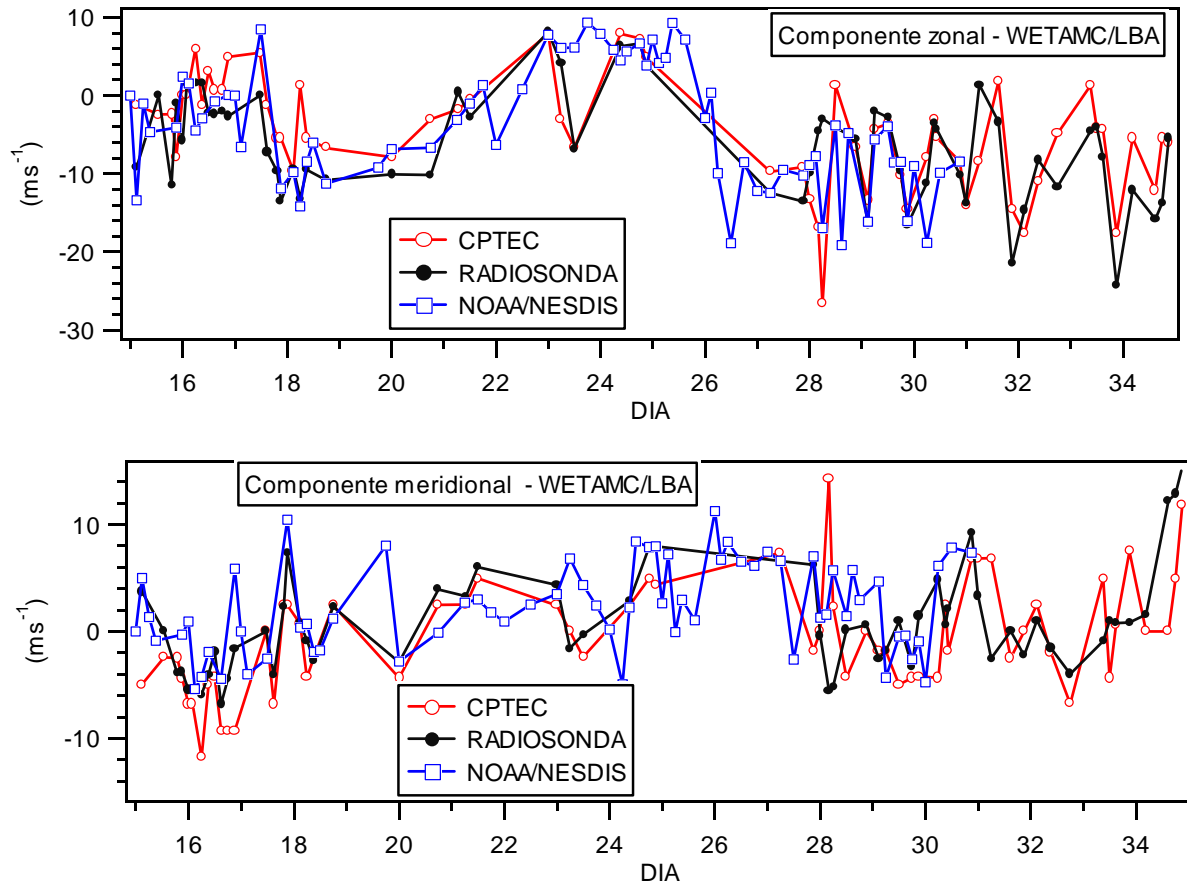
The correction reduced the error in the level estimate for high and middle level winds (levels in which semi-transparent clouds can be identified). The statistics in the wind comparison with the NOAA/NESDIS vectors did not change in the total, because they are the same vectors. Only there are small differences due to change of a part of middle vectors for high levels. The number of wind vectors in high levels increases around 14 %. With application of this correction, the BIAS of the pressure changed from 28 hPa to -2 to the highest levels, and decreased from 59 hPa to 24 hPa for the middle levels. However this correction does not affect the low vectors ( $P > 700$  hPa).

Table 5 shows the results obtained when the spatial consistency test is not applied. The effect of this test is to remove about 12% of the vectors, carrying in RMS reduction from  $7.1 \text{ ms}^{-1}$  to  $5.9 \text{ ms}^{-1}$  in the total. It can be noted that the reference velocity did not decrease (in a opposite way it increased lightly), that means that the space consistency test effect does not reject the high-speed vectors but actually rejects spatially inconsistent vectors.

	CPTEC (without spatial consistency test) x NOAA/NESDIS			
	All levels	$P > 700$ hPa	$400 < P < 700$ hPa	$P < 400$ hPa
Difference Mean Vector	1.7	1.4	1.6	1.8
Difference Mean Vector RMS	7.4	7.2	7.6	7.4
Velocity BIAS	-0.4	-0.2	-0.3	-0.5
Difference RMS	4.4	4.1	4.6	4.5
Mean velocity of reference	10.1	9.8	10.0	10.3
Pressure BIAS	24	57	41	-4
Pressure RMS	169	218	207	101
Sample size	73392	17014	22072	34306

**Table 5.** Same as Table 3, but CPTEC vectors were calculated without spatial consistency test.

The vectors extracted from satellite images were compared with the wind measured by radiosonde in the corresponding level ( maximum difference of 15 hPa). Figure 1 presents the temporal evolution of zonal and meridional wind components measured by a radiosonde station and winds calculated by CPTEC and NOAA/NESDIS. We observe a good coherence between the different wind vector estimates.



**Figure 1.** Zonal and meridional Wind components observed in the ABRACOS (10.77 S – 62.34 W) radiosonde station and the Wind obtained by satellite in CPTEC and NOAA/NESDIS during AMC/LBA. Curves represent the vector components calculated by CPTEC and NOAA/NESDIS, and Wind components measured by radiosonde at the corresponding pressure level.

A wind vector evaluation from radiosonde data is presented in Tables 6 and 7.

	CPTEC x Radiosonde			
	All levels	P > 700 hPa	400 < P < 700 hPa	P < 400 hPa
Difference Mean Vector	2.7	23.4	0.9	3.5
Difference Mean Vector RMS	7.5	24.8	7.8	6.5
Velocity BIAS	-1.7	-15.1	-2.9	-2.5
Velocity Difference RMS	5.3	15.8	4.8	4.9
Reference Mean Velocity	10.6	8.3	4.4	11.3
Sample size	147	3	13	131

**Table 6.** Statistical Wind differences ( $\text{ms}^{-1}$ ) between CPTEC and radiosonde vectors. BIAS is the mean difference and RMS is the root mean square.

NOAA/NESDIS x Radiosonde				
	All levels	P > 700 hPa	400 < P < 700 hPa	P < 400 hPa
Difference Mean Vector	1.3	0.82	1.2	1.3
Difference Mean Vector RMS	6.2	4.9	4.0	6.3
Velocity BIAS	-0.7	0.7	3.3	-0.8
Velocity Difference RMS	3.6	2.0	3.4	3.7
Reference Mean Velocity	10.0	4.7	3.1	10.4
Sample size	158	3	6	149

**Table 7.** Same as Table 6, but for NOAA/NESDIS vectors.

The experiment period was dominated by high clouds, resulting in a reduced number of satellite measurements for middle and low level clouds. Therefore the results are not significant for these levels. For the high level (P < 400 hPa) the CPTEC vectors have a RMS of  $6.5 \text{ ms}^{-1}$  and BIAS of  $-2.5 \text{ ms}^{-1}$  for a mean velocity of  $11.3 \text{ ms}^{-1}$ . The NOAA/NESDIS vectors have RMS of  $6.3 \text{ ms}^{-1}$  and BIAS of  $-0.8 \text{ ms}^{-1}$  for mean velocity of  $10.4 \text{ ms}^{-1}$ .

These results show a similar performance for both methods. In the lowest levels we cannot conclude, but the few data (3 in low levels and 13 in middle levels) suggest that the CPTEC vectors are not so good, and must be improved.

## 5. Operational Product Evaluation – DSA/CPTEC.

Wind fields estimates based in clouds displacement using geostationary satellites images started to being produced 8 times a day in September 2000 at the DSA/CPTEC. A wind field example in three levels obtained in CPTEC operational outline for December 30<sup>th</sup> 2000 is presented in **Figure 2**. It can be noted a large number of vectors with a good space consistency. An incorrect estimate example can be seen in the region (10 N-35 W) where three wind vectors representative of the high or middle troposphere wind were estimated as low levels wind.



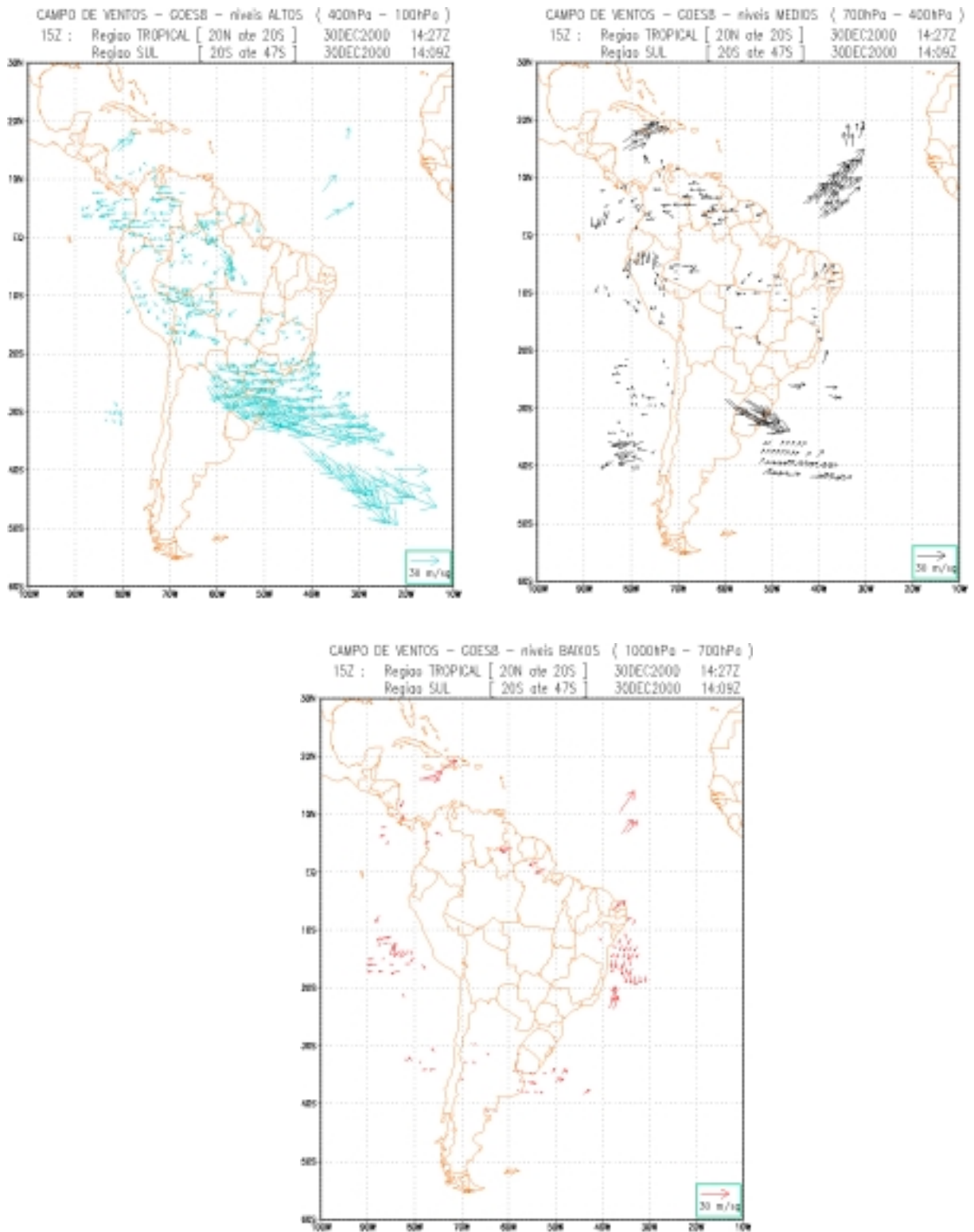


**Figure 2.** Wind fields from GOES-IR images using DAS/CPTEC's operational scheme for December 30<sup>th</sup> 2000 at 14:00 GMT. Wind Fields are showed in three levels.

Several improvements were done in the original algorithm, aiming to get more consistent and reliable results; one could cite among others the cloud semi-transparency correction and the spatial consistency test. As observed in the previous section, the results obtained from the data comparison between the algorithm and radiosonde data observed during the WETAMC/LBA experiment showed satisfactory performance. The results were obtained in extremely favorable conditions, having in mind that the GOES data used were obtained directly from NOAA/NESDIS, which could guarantee a certain data "quality" (even so with problems in about 8% of the images). Radiosonde data were obtained for a specific experiment, using an only radiosonde system, which propitiates better consistency and quality in the observations. In an experiment of this kind the collocations between satellite and radiosonde data can be better defined than in an operational outline, where the radiosonde location and launching time schedules usually are not coincident.

As an example a comparison between wind fields obtained operationally at DSA/CPTEC and radiosonde data for December 2000 is presented in Table 8.

	DSA/CPTEC x Radiosonde			
	All levels	P > 700 hPa	400 < P < 700 hPa	P < 400 hPa
Difference Mean	3.3	3.5	2.4	3.9
Vector				
Difference Mean	9.5	10.3	8.6	9.5
Vector RMS				
Velocity BIAS	-0.6	0.5	1.6	-2.1
Velocity difference	6.1	4.9	5.3	6.8
RMS				
Reference Mean	9.2	7.8	6.5	11.1
Velocity				
Sample size	178	44	41	93

**Table 8.** Wind statistical differences ( $m.s^{-1}$ ) between DAS/CPTEC operational vectors and radiosonde data. BIAS is the mean difference and RMS is the root mean square.

Results obtained in the Table 8 are affected by problems like frequency in the images availability, having in mind that NOAA/NESDIS does not transmit images for the south sector when operating in the "rapid scan" mode, in this case the methodology which uses a sequence of three consecutive images can not be performed.

For example during December 2000 in a total of 717 possible images, were actually available 366 images, performing a total of 51% useful images. This loss must be credited jointly to problems in transmitted images by NOAA/NESDIS (note that during the experiment WETAMC/LBA the percentile of images with problems was of about 8%); and images loss due to problems in the reception at DSA/CPTEC station.

Must be considered also that some radiosonde stations presented systematically large differences regarding the algorithm results, values which in a more detailed analysis showed unlikely with regard to the vertical structure of the sounding.

Other observed fact was the occurrence of vectors groups with opposite direction related to the wind flow in a same level. More accurate analysis of some particular situations showed a very strong wind shear in a thin atmospheric layer, indicating that however these vectors had been placed in a same level, in fact they were in different levels but next to each other. This kind of problem tends to disappear with a better estimate in clouds height.

It was observed also that semi-transparency correction sometimes does not perform well, mostly when there is confusion between high clouds and low clouds. This problem can be minimized with a better thresholds definition, that will be established through a specific analysis for this kind of situation.

Most of previously presented problems should be minimized with a more precise cloud classification scheme.

## **6. Conclusion**

A new version for wind extraction from satellite image has been tested in CPTEC. Two main improvements were developed: a semi-transparent cloud height correction, using an original radiative model; and a spatial consistency filter. The radiative model was validated using a line-by-line model. The vectors produced with the new CPTEC drift wind version were compared with the vectors produced by NOAA/NESDIS, recognized trustful source, to analyze the functioning of the methodology and the modification effect. As foreseen, semitransparency correction allows to improve the wind vectors height assignment in high levels. The space consistency filter has a strong impact, improving the statistics for all levels. The vectors from the CPTEC model become as good as the vectors from NOAA/NESDIS for high levels. This result is promising because NOAA/NESDIS vectors were already adjusted using a forecast model. For the middle and low levels the results indicate that the CPTEC vectors are not so good, however the statistical population was too small to derive definitive conclusions. With regard to the comparison with WETAMC/LBA radiosonde data the results show that RMS are similar for both models and present satisfactory results for the high levels.

The CPTEC cloud drift performance for the operational outline is limited by some basic problems like problems in image transmission, problems in the CPTEC reception system, and noise in NOAA/NESDIS transmitted images, like described in section 5. Additional to these problems it was verified that some radiosonde stations presented problems in data consistency. As the comparison period was too short (1 month), it is expected that the analysis of a longer period, the images quality control and a depuration in radiosonde data could allow improvements in the performance of the operational scheme.

We suggest that the improvements for a next phase can be focused in the implantation of better cloud classification, aiming to improve the winds quality in low levels.

## **Acknowledgments**

The authors thank J. M. Daniels (NOAA/NESDIS) for furnishing the high-resolution satellite wind dataset produced during the experiment.

Thanks to the AEB – (Agência Espacial Brasileira) for support Nelson Arai's research activities.

This work was part of cooperation between IRD (Institut de Recherche pour le Développement, France) and CNPq (Conselho Nacional de Desenvolvimento Científico e Tecnológico) support number 910153/98-1. This work was also partially financed by FAPESP (Fundo de Amparo 'a Pesquisa do Estado de São Paulo) support number 99/06045-7.

## REFERENCES

- BOWEN, R. L., SAUNDERS, R. The semi transparency correction as applied operationally to Meteosat infrared data: a remote sensing problem. *European Space Agency Journal*, Darmstadt, n.8, 125-131, 1984.
- CLOUGH, S. A., KNEIZYS, F. X., DAVIES, R. W. Line shape and the water vapor continuum. *Atmospheric Research*, v.23, 229-241, 1989.
- CHOU, M. D., LEE, K. T. Parameterizations for the absorption of solar radiation by water vapor and ozone. *Journal of the Atmospheric Sciences*, v.53, n.8, 1203-1208, 1996.
- EUMETSAT. Proc. of the fourth International Winds Workshop, Saanenmoser, Switzerland, 20-23 October 1998. Eumetsat Publ. EUM P 24, 322 pp, 1998.
- FEIGELSON, E. M., FOMIN, B. A., GORCHAKOVA, I. A., ROZANOV, E. V., YU, TIMOFEYEV, M., TROTSENKO, A. N., SCHWARZKOPF, M. D. Calculation of longwave radiation fluxes in atmospheres. *Journal of Geophysical Research*, v.96, n.5, 8985-9001, 1991.
- FOMIN, B. A. Effective interpolation technique for line-by-line calculations of radiation absorption in gases. *Journal of Quantitative Spectroscopy and Radiative Transfer*, v.53, n.6, 663-669, 1995.
- KALNAY, E., ET AL. The NCEP/NCAR 40-year reanalysis project. *Bulletin of American Meteorological Society*, v.77, n.3, 437-471, 1996.
- LAURENT, H., MACHADO, L. A.. Extração de vento através de imagens de satélite meteorológico. *Anais do VIII Congresso Brasileiro de Meteorologia*, Belo Horizonte (MG), SBMET, 18 a 25 de outubro de 1994, v.1, 410-413, 1994.
- LIU K. N. Radiation and cloud processes in the atmosphere. Theory, observation and modeling, New York. Oxford., Oxford University Press. Pp.486, 1992.
- MENZEL W. P., SMITH, W. L., STEWART, T. R. Improved cloud motion wind vector and altitude assignment using VAS. *Journal of Climate and Applied Meteorology*, v.22, n.3, 377-384, 1983.
- NIEMAN S. J., MENZEL, W. P., HAYDEN, C. M., GRAY, D., WANZONG, S. T., VELDEN, C. S., DANIELS, J. Fully automated cloud-drift winds in NESDIS operations. *Bulletin of American Meteorological Society*, v.78, n.6, 1121-1133, 1997.
- RIDGWAY, W. L., HARSHVARDHAN, ARKING, A. Computation of atmospheric cooling rates by exact and approximate methods, *Journal of Geophysical Research*, v.96, n.5, 8969-8984, 1991.
- ROBERTS, R. E., SELBY, J. E. A., BIBERMAN, L. M. Infrared continuum absorption by atmospheric water vapor in the 8-12  $\mu\text{m}$  window. *Applied Optics*, v.15, n.9, 2085-2090, 1976.
- ROTHMAN, L. S., ET AL. The HITRAN molecular database and HAWKS, 1996 edition, *Journal of Quantitative Spectroscopy and Radiative Transfer*, v.60, 665-710, 1998.
- SCHMETZ, J., HOLMLUND, K., HOFFMAN, J., STRAUSS, B., MASON, B., GAERTNER, V., KOCH, A., VAN DE BERG, L. Operational Cloud-Motion Winds from Meteosat Infrared Images. *Journal of Applied Meteorology*, v.32, n.7, 1206-1225, 1993.
- SILVA DIAS M.A.F. Experimento de grande escala da interação biosfera atmosfera na Amazônia: resultados preliminares. *Boletim da Sociedade Brasileira de Meteorologia*, v.25, n.1, 7-14, 2001.
- SILVA DIAS M.A.F., RUTLEDGE, S., KABAT, P., SILVA DIAS, P., NOBRE, C., FISCH, G., DOLMAN, H., ZIPSER, E., GARSTANG, M., MANZI, A., FUENTES, J., ROCHA, H., MARENGO, J., PLANA-FATTORI, A., SÁ, L., ALAVALÁ, R., ANDREAE, M., ARTAXO, P. Clouds and rain processes in a biosphere atmosphere interaction context in the Amazon region. *Journal of Geophysical Research*, in press, 2002.